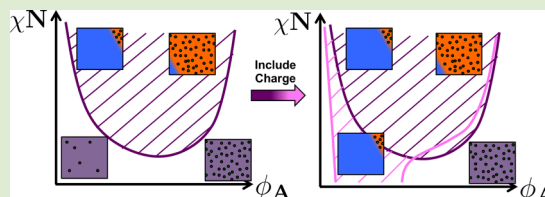


## Ion Correlation-Induced Phase Separation in Polyelectrolyte Blends

Charles E. Sing, Jos W. Zwanikken, and Monica Olvera de la Cruz\*

Department of Materials Science and Engineering, Northwestern University, Evanston, Illinois 60208, United States

**ABSTRACT:** Inhomogeneous polyelectrolyte materials have been of both longstanding and recent interest; polymer blends exhibit technologically advantageous properties for adhesives and fuel cell membranes and serve as an ideal model system to study more complicated behaviors in polyelectrolyte materials. However, the physics governing the phase behavior of polyelectrolyte blends remains poorly understood. Traditional self-consistent field theory (SCFT) can include Coulombic interactions that arise in polyelectrolytes but can only reproduce Poisson–Boltzmann behavior or perturbations thereof due to the mean-field nature of the SCFT calculation. Recently, tools have been developed to couple SCFT with liquid state (LS) integral equation theory, which can calculate ion correlations in a quantitative fashion. This permits the articulation of ion effects in very low dielectric  $\epsilon_r$  constant regimes that are relevant to polymer blends in nonaqueous conditions. We show that the inclusion of local ion correlations can give rise to marked enhancement of phase separation, contrary to theories invoking the Poisson–Boltzmann approximation, even to the extent of driving phase separation when two polymers are fully miscible ( $\chi N = 0$ ). We provide both a demonstration of this effect as well as a conceptual explanation.



Blends involving at least one polyelectrolyte species are of great technological interest, as they provide a facile way to combine the advantageous properties of two polymers in a single material. A wide range of physical systems have been realized experimentally; in the solution phase, for example, pairs of oppositely charged polyelectrolytes drive highly controlled layer by layer systems for structured membranes,<sup>1</sup> and complex coacervate systems have been investigated as biomimetic adhesives.<sup>2</sup> Blends are also important in the melt phase. A class of polyelectrolytes that have low charge fractions, known as “ionomers,” have been studied extensively in both single-component<sup>3,4</sup> and blend systems<sup>5–7</sup> due to their promise as fuel cell membranes due to the relative success of the commercial ionomer Nafion<sup>5,8</sup> as well as their ability to enhance the mechanical and barrier properties of the nonionomer blend component.<sup>7</sup> Experimental and simulation studies have demonstrated that local structural information is important in the phase behavior of such materials.<sup>3,4,6</sup> While blending with specific complementary moieties will result in enhanced miscibility,<sup>7</sup> immiscibility is usually enhanced by the presence of backbone charges in ways that are counterion-dependent.<sup>5,6</sup> Polymer blends also serve as an important model system for the understanding of the thermodynamics of more complex systems, with blend literature<sup>9</sup> providing the language to articulate related fields such as block copolyelectrolytes<sup>10</sup> that are widely considered for applications in stimuli-responsive materials and battery membranes.<sup>11,12</sup> Despite their relevance, there is very little theoretical research into the phase behavior of melt polyelectrolyte blends, with existing work focused on using phase behaviors of blends as a model system for block copolymer systems.<sup>13,14</sup>

Historically, self-consistent field theory (SCFT) studies on polyelectrolytes have utilized the Poisson–Boltzmann (PB)

approximation,<sup>10,15,16</sup> despite the well-known result that such methods are severely limited in terms of the strength of the ion coupling.<sup>16</sup> In fact, even elaborate perturbation methods yield results that are only applicable to monovalent ions in an aqueous environment, which is far weaker than the charge coupling between ions in the blend-relevant case of ions in the extremely low dielectric environment of polymer melts or blends.<sup>16</sup> Building off work in two-phase gel systems,<sup>17</sup> we have recently developed a self-consistent thermodynamic model capable of describing the behavior of polyelectrolyte systems that incorporates the liquid state (LS) integral equation theory into standard SCFT methods such that inhomogeneous polyelectrolyte systems are described in a fashion that considers the effect of charge correlations.<sup>18</sup> Thus, local structure that is known to be important in experiments can be theoretically articulated.<sup>3,18</sup> LS theory provides a thorough description of correlations by comparing an infinite number of terms in Mayer cluster expansions.<sup>19</sup> This comparison is approximate, as many clusters are neglected in making this comparison (primarily “bridge diagram” contributions);<sup>19</sup> however, even in highly coupled electrolytes comparison to simulation is quantitative in most regimes of interest.<sup>20</sup>

We use this theoretical tool to investigate the phase behaviors of polyelectrolyte blends and demonstrate that correlation effects can be incredibly important; existing theories on related block copolymer systems neglect these effects and observe a suppressed phase separation,<sup>21–23</sup> while we predict that the inclusion of correlations will demonstrate the opposite behavior in a blend of polyelectrolytes. Our results are in line

**Received:** October 3, 2013

**Accepted:** November 6, 2013

**Published:** November 8, 2013

with experimental observations, which typically observed charge-induced enhancement of phase separation in both blends and block copolymers.<sup>5,6,24</sup> Realizing conditions appropriate for polymer melts (relative dielectric constants  $\epsilon_r \sim 5\text{--}10$  and ion sizes  $a = 2.5 \text{ \AA}$ ), it is even possible to observe phase separation in blends that are otherwise completely miscible ( $\chi N = 0$ ).

We consider a blend of two polymers of length  $N$ , an  $A$  polymer that has a fraction  $f_q$  of charged monomers, and a  $B$  polymer that is uncharged. There are short-ranged repulsions between the monomers of  $A$  and  $B$  that are represented by the classical Flory–Huggins  $\chi$ -parameter. We consider these polymers to be the sole components in a SCFT calculation, using a coordinate grid  $\mathbf{x}$  that is discretized by units  $\Delta \mathbf{x} \sim 10\text{--}100 \text{ nm}$ . This is governed by the well-known free energy functional  $\mathcal{F}_{\text{SCFT}}$ :<sup>10,15</sup>

$$\frac{\mathcal{F}_{\text{SCFT}}}{k_B T}[\omega_-, \omega_+, \mu_{\text{CORR}}] = \rho_0 \int \frac{\omega_-^2}{\chi} - i\omega_+ d\mathbf{x} - n \ln Q[\omega_A] - n \ln Q[\omega_B] \quad (1)$$

where  $n$  is the number of polymers in the system;  $\rho_0 = nN/V$  is the monomer density; and  $\omega_-$  and  $\omega_+$  are the conjugate fields that are solved for self-consistently for the equilibrium values  $\omega_{\pm}^*$  such that  $(\delta \mathcal{F}_{\text{SCFT}}/\delta \omega_{\pm})_{\omega_{\pm}^*} = 0$  and  $(\delta \mathcal{F}/\delta \omega_{\pm})_{\omega_{\pm}^*} = 0$ .<sup>15</sup> In this model,  $\omega_{A/B} = \mp \omega_{\pm} - i\omega_+ + f_q \delta_A (\ln(\rho_{\pm}) + 2\mu_{\text{CORR}})$  are the fields (the subscript  $A/B$  denotes that there are two equations for  $A$  and  $B$  that have the same form but different signs  $\mp$ ) that are included in the single-chain partition functional  $Q = \int d\mathbf{x} q(\mathbf{x}, s = N)$ , which is calculated upon solving the diffusion equation  $\partial q_{A/B}(\mathbf{x}, s)/\partial s = [b^2/6 \nabla^2 - \omega_{A/B}]q(\mathbf{x}, s)$  where  $b$  is the monomer length and  $q$  is the single chain propagator.<sup>15</sup> The contribution  $f_q \delta_A (\ln(\rho_{\pm}) + 2\mu_{\text{CORR}})$  is the field due to the presence of the charged monomers (the  $\delta_A$  denotes that this only applies for the charged species); it describes their interactions with each other as well as the surrounding counterions (that have concentration  $\rho_{\pm}$ ).<sup>18</sup>

Within each SCFT grid point,  $\Delta \mathbf{x}$ , we consider the local structure to be a homogeneous, electroneutral liquid of counterions of radius  $a$  with density  $\rho_{\pm}$  and charged monomers  $\rho_{\pm} = \rho_0 \phi_A f_q = \rho_{\pm} = \rho_{\pm}$ .<sup>25</sup> We will only consider monovalent ions  $z = 1.0$ . The organization of these charges is dictated by the Coulombic interactions and the hard-sphere repulsions of these components (since we focus on low  $f_q$  we for now assume that we can neglect charge connectivity on this local level). This organization is characterized by the pair correlation function  $g(r) = h(r) + 1$ , which can be calculated directly using LS theory.<sup>19,20</sup> In LS theory, only the densities  $\rho_{\pm}$  and the pairwise potential  $u$  between two entities are necessary to determine  $g(r)$ .<sup>19</sup> In our situation, the pair potential between charged species  $i$  and  $j$  is given by  $u_{ij} = k_B T z_i z_j \lambda_B / r + u_{\text{HC}} \Theta(2a - r)$ , where  $u_{\text{HC}} \rightarrow \infty$  is the hard core potential whose range is set by the Heaviside function  $\Theta(2a - r)$  and  $\lambda_B = e^2/(4\pi\epsilon k_B T)$  is the Bjerrum length ( $e$  is the electron charge, and  $\epsilon$  is the dielectric constant).  $u_{ij}$  and  $\rho_{\pm}$  are placed into two equations: the Ornstein–Zernike equation  $\hat{\mathbf{h}}_{ij} = \hat{\mathbf{c}}_{ij} + \rho_{\pm} \hat{\mathbf{c}}_{ik} \hat{\mathbf{h}}_{kj}$  (hats denote Fourier transformed values, indices denote different charged species  $i, j, k = \{+, -\}$ ) and a closure relation that independently links  $\mathbf{c}_{ij}$  and  $\mathbf{h}_{ij}$ .<sup>19</sup>  $\mathbf{h}_{ij} = \mathbf{g}_{ij} - 1.0$  is the total correlation function (related to the pair correlation function  $\mathbf{g}_{ij}$ ) between  $i$  and  $j$ , while  $\mathbf{c}_{ij}$  is the direct correlation function.<sup>19</sup> We

note that both of these functions are typically radially symmetric for spherical ions, with a coordinate  $\mathbf{r}$  that is on a much smaller length scale than  $\mathbf{x}$ . In this work we use the Debye–Huckel extended mean spherical approximation (DHMSA) closure relationship, which is described in Zwanikken et al.<sup>20</sup> It is essentially identical in most situations to the well-known hypernetted chain (HNC) closure, and both are known to reproduce simulation data nearly quantitatively.<sup>20</sup> Also, using HNC we can calculate the correlation-based chemical potential of a given ion  $\mu_{\text{CORR},i}$  that is not associated with the ideal gas chemical potential  $\mu_{\text{IG}} = \ln(\rho_{\pm})$ <sup>17–19</sup>

$$\mu_{\text{CORR},i} = \sum_{j=\pm} \frac{\rho_j}{2} \int d\mathbf{r} \mathbf{h}_{ij}[\mathbf{h}_{ij} - \mathbf{c}_{ij}] - \rho_j \int d\mathbf{r} \mathbf{c}_{ij} \quad (2)$$

While this is strictly relevant only for the HNC closure,<sup>19</sup> DHMSA is known to be nearly identical, and we will use this expression.<sup>20</sup> It is this chemical potential that is included in the single chain partition functional calculation in eq 1. The iterative technique we use is described in more detail in Sing et al.,<sup>18</sup> however, the concept of the approach is that we calculate  $\mu_{\text{CORR}}$  at every grid point  $\mathbf{x}$  based on the density  $\rho_{\pm}$  at each location. This density is based on the density of  $A$  and  $B$  calculated from  $Q^*[\omega_{\pm}^*, \mu_{\text{CORR}}]$

$$\rho_{A/B}[Q^*] = -n \frac{\delta \ln Q[\omega_{\pm}^*, \mu_{\text{CORR}}]}{\delta(\mp i\omega_{\pm})} \quad (3)$$

This in turn is dependent on the correlation chemical potential  $\mu_{\text{CORR}}$  of the charged species. This dependency is iteratively carried out until  $\mu_{\text{CORR}}$  and  $\rho_{A/B}$  are self-consistent. Figure 1 schematically describes our scheme and the coupling between the large polymer-length scales  $\mathbf{x}$  and the small charge-correlation length scales  $\mathbf{r}$ .

The new parameter in this method is the introduction of the correlation chemical potential  $\mu_{\text{CORR}}$  as the bridge between the coarse-grained representation of the inhomogeneous polymer

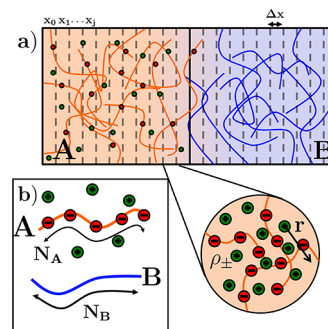


**Figure 1.** (a) Schematic demonstrating the system of interest, with two length scales. A large length-scale grid (bottom square) is considered with a 1-dimensional coordinate  $\mathbf{x}$  that is divided into regions of size  $\Delta \mathbf{x}$ . The behavior of polymers on this length scale is determined by SCFT, which can demonstrate the creation of phase-separated  $A$ - and  $B$ -rich regimes. Each of these grid regions is demonstrated on a smaller length scale by a homogeneous fluid of charges (magnified circle) with one of the species being the counterions and the other species being the backbone charges. Within the area  $\Delta \mathbf{x}$ , distances are given by the coordinate  $r$  along which correlations are calculated using LS theory. (b) Charged polyelectrolyte chains  $A$  and neutral polymer chains  $B$  are considered in this work.  $A$  and  $B$  chains of length  $N$  have short-range interactions given by  $\chi$  and  $A$  containing a fraction of charged monomers  $f_q$ .

system described by the SCFT calculation and the molecular-level correlation data described by LS theory.<sup>17,18</sup> This chemical potential will not be constant in space, as it depends on the local concentration of the charged species  $\rho_{\pm}$ . In an *A* homopolymer phase, we can plot this chemical potential contribution as a function of the fraction of charge  $f_q$ . This represents the energy associated with a single ion in a homogeneous fluid of ions with a fraction that is related to the charge density  $\rho_{\pm} = f_q \rho_0$  and can be plotted for a number of different values of the normalized Bjerrum length  $\Gamma = \lambda_B/(2a)$ . In an aqueous environment,  $\Gamma \approx 1$ , and thus the distance over which the Coulombic interaction is greater than thermal energy is approximately the distance between ions, which permits the use of Poisson–Boltzmann in these situations. This is much weaker than the case of a melt of polymer, which may have extremely low relative dielectric constants  $\epsilon_r \approx 5$ –20 (compared to water  $\epsilon_r = 80.1$ ). For this work, we consider both *A* and *B* to have equivalent  $\epsilon_r$  to separate this effect from self-energy effects described by Wang.<sup>13</sup> This is well-motivated, since except for a few outliers such as PEO ( $\epsilon_r = 7.5$ )<sup>13</sup> most technologically relevant polymers have nearly identical  $\epsilon_r \sim 2.5$ –4 and situations where self-energy effects are small are likely.<sup>26</sup> Even in situations where self-energy effects are pronounced, this effect remains significant. We therefore consider values of  $\Gamma \approx 4.5$ –22.5, corresponding to highly coupled charges. The weakest Coulombic interaction  $\Gamma \approx 4$  is similar in strength to divalent ions in an aqueous environment, which are already known to be poorly described by perturbation theories.<sup>16</sup> We plot  $\mu_{\text{CORR}}$  for a number of values  $\Gamma$  in Figure 2, which is for a homogeneous, charged (*A*) polymer of charge fraction  $f_q$  (or an effective charge fraction  $f_q \rightarrow f_q \phi_A$  for a mixture). The qualitative behavior of this plot reveals the role of ion correlations in highly interacting polymer systems. In the limit of low charge fraction  $f_q \rightarrow 0$  a single ion tends to the limit  $\mu_{\text{CORR}} \rightarrow 0$ . This is the limiting case of ideal

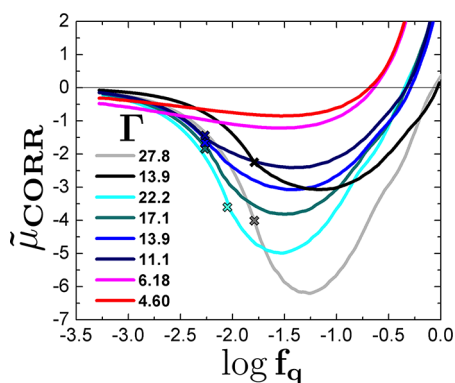


**Figure 2.** Chemical potential  $\tilde{\mu}_{\text{CORR}}$  for the charged species in a polyelectrolyte melt as a function of the fraction of charged monomers  $f_q$  (monovalent, with an equal number of monovalent counterions). A number of values of correlation strength  $\Gamma = \lambda_B/(2a)$  are shown, representing a variety of values of the relative dielectric constant  $\epsilon_r$  and ion radius  $a$ . Three ion radii are represented:  $a = 2.0$  Å (black/gray),  $a = 2.5$  Å (blue/green), and  $a = 3.0$  Å (red/pink). These values are calculated using the DHEMSA closure, which becomes unstable at densities below the indicated points (crosses). Linear extrapolation from these points to the limit of  $\mu_{\text{CORR}} \rightarrow 0$  as  $f_q \rightarrow 0$  follows; we do not expect this approximation to have profound effects on the results of this article. Chemical potentials can be as large as  $6 - 7k_B T$  for the largest value of  $\Gamma$  shown. All values of  $\Gamma$  are realistic for ions in polymer melts.

gas behavior at low concentrations, which is expected for any system at sufficient dilution. As  $f_q$  increases,  $\mu_{\text{CORR}}$  becomes significantly less than 0 ( $\mu_{\text{CORR}} \ll 0$ ,  $|\mu_{\text{CORR}}| \gg 1k_B T$ ) such that at intermediate ion concentrations the tendency of oppositely charged ions to attract lowers the energy of the system with increasing concentrations of ions. This also informs our use of the  $\Gamma$  parameter, as we plot  $\Gamma = 13.9$  for  $a = 2.5$  and  $2.0$  Å ( $\epsilon_r = 10.0$  and  $8.0$ , respectively), and both have the same minimum in  $\tilde{\mu}_{\text{CORR}}$ . While this effect is strong, at some point the excluded volume of the ions becomes significant. At large charge fractions  $f_q > 0.1$ –0.2,  $\mu_{\text{CORR}}$  begins to increase significantly. This is due to the entropic penalty paid by the presence of large ions, as they exclude volume that lowers the amount of configurational entropy in the dense charged system.<sup>18</sup> The significance of this behavior is that at intermediate  $f_q$  the charged polymer is highly attracted to itself; however, this is suppressed at high values of  $f_q$  due to excluded volume.

These thermodynamic behaviors are relevant to the phase behavior of polyelectrolyte blends, where one of the polymers is charged and the other is not ( $f_q > 0$ ). We can calculate the phase behavior using SCFT, which we indicate in Figure 3 for a

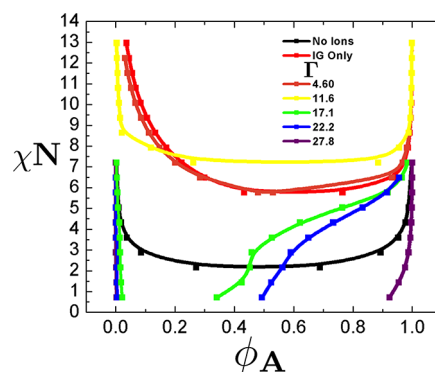


**Figure 3.** Phase diagram on the  $\chi N$ – $\phi_A$  plane from a number of charge-neutral polymer blends. The mean-field Flory–Huggins result for a symmetric blend (black) has a theoretically predicted  $\chi_{\text{critical}} N = 2.0$ . Above this binodal, there is a coexistence regime where phase separation occurs. The inclusion of *only* the ideal gas contribution of the counterions ( $\mu_{\text{CORR}} = 0$ ) results in the red curve, which demonstrates strongly suppressed phase separation such that  $\chi_{\text{critical}} N \approx 5$ –6. Inclusion of correlations with a strength denoted by  $\Gamma$  enhances phase separation at large  $\Gamma$  in contrast to the ideal gas result. At large values of  $\Gamma \geq 17$  phase separation is observed even at  $\chi N = 0$  indicating that charge correlations alone can drive phase separation.  $f_q = 0.1$  and  $N = 40$ ,  $a = 3.0$  Å for  $\Gamma = 4.6, 11.6$ ,  $a = 2.5$  Å for  $\Gamma = 17.1, 22.2$ , and  $a = 2.0$  Å for  $\Gamma = 27.8$ .

number of situations ( $N = 40$  for all results). In Figure 3, we plot the phase behavior for an uncharged symmetric system (black) which corresponds to the well-known Flory–Huggins mean-field result ( $\chi_{\text{critical}} N = 2.0$ ). For all plots, the phase-separated region is above the binodal lines. If charges are included such that only the ideal-gas behavior is considered ( $\mu_{\text{CORR}} = 0$ ), the red curve is obtained; this demonstrates significant suppression of the phase separation to large values of  $\chi N > 5$ –6, an effect that occurs more significantly on the left side of the diagram. This is due to the decrease in ion entropy concomitant with phase separation since it is entropically favorable for the system to be in a mixed state where the counterions are free to sample configurations spanning the entire sample. This is in qualitative agreement with literature observations in the related block copolymer theoretical

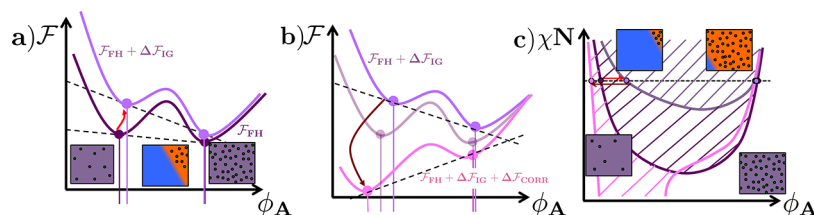


**Figure 4.** (a) Schematic of the free energy curve  $\mathcal{F}_{\text{FH}}$  (purple) versus  $A$ -polymer fraction  $\phi_A$  from the Flory–Huggins theory of homopolymer mixing. A common tangent construction evaluates the binodal. Inclusion of the translational entropy of the counterions results in a shift of this curve to  $\mathcal{F}_{\text{FH}} + \Delta\mathcal{F}_{\text{IG}}$  (light purple), resulting in a decrease in the regime of phase separation. (b) Similar curves to (a), only now including the shift due to charge correlations  $\mathcal{F}_{\text{FH}} + \Delta\mathcal{F}_{\text{IG}} + \Delta\mathcal{F}_{\text{CORR}}$  (pink) that drastically decreases the free energy of the low- $\phi_A$  free energy. This leads to an enhancement in phase separation, as demonstrated. Corresponding phase behavior is indicated along the dotted line in (c), which shows the shifts of (a) and (b). Diagrams demonstrate why effects are more drastic at low  $\phi_A$ ; the difference between the phase-separated and mixed states at high  $\phi_A$  is minimal, while such differences are significant at low  $\phi_A$ .

literature, which does not include correlations.<sup>15,21–23</sup> The inclusion of weak correlations ( $\Gamma = 4.6$ ) changes this diagram very little; however, further increase in the strength of the correlation results in a significant increase in phase separation. At  $\Gamma = 17.1$ , which corresponds to ions of size  $a = 2.5 \text{ \AA}$  in a dielectric constant of  $\epsilon_r = 6.5$ , phase separation at values of  $\phi_A$  occurs even at  $\chi N = 0$ . This effect only increases upon increasing  $\Gamma$ . We therefore predict that phase separation can be induced solely by the charge correlations even in the absence of short-range (i.e., dispersive,  $\chi$ -induced) immiscibility.

The behaviors described in the phase diagrams are conceptually understandable based on consideration of corrections to Flory–Huggins mean field theory. Without charges, a symmetric polymer blend has the Flory–Huggins free energy  $\mathcal{F}_{\text{FH}}$

$$\frac{\mathcal{F}_{\text{FH}}(\phi_A)}{Vk_B T} = [\phi_A \ln \phi_A + (1 - \phi_A) \ln(1 - \phi_A)]/N + \chi \phi_A (1 - \phi_A) \quad (4)$$

With charges, the free energy will include corrections due to ideal gas confinement to the  $A$ -rich phase  $\Delta\mathcal{F}_{\text{IG}}(f_q, \phi_A) \approx \mathcal{F}_{\text{IG}}(\phi_A \approx 1) - \mathcal{F}_{\text{IG}}(\phi_A)$  and due to correlation enhancement upon confinement to the  $A$ -rich phase  $\Delta\mathcal{F}_{\text{CORR}}(f_q, \phi_A) \approx \mathcal{F}_{\text{CORR}}(\phi_A \approx 1) - \mathcal{F}_{\text{CORR}}(\phi_A)$ , such that the actual free energy is given by  $\mathcal{F}_{\text{TOT}} = \mathcal{F}_{\text{FH}} + \Delta\mathcal{F}_{\text{IG}} + \Delta\mathcal{F}_{\text{CORR}}$ . For the ideal gas term, the counterion entropy is given by  $\mathcal{F}_{\text{IG}}(\phi_A, f_q) = f_q \phi_A \ln(\phi_A f_q)$ , so  $\Delta\mathcal{F}_{\text{IG}}(\phi_A, f_q) \approx -f_q \phi_A \ln \phi_A > 0$ , which increases the free energy. This increase happens primarily at low values of  $\phi_A$ , as is demonstrated schematically in Figure 4a. This increase results in a concomitant shift in the phase boundary such that the phase separation regime is suppressed. The correlation term is given by  $\mathcal{F}_{\text{CORR}} \approx 2f_q \phi_A \mu_{\text{CORR}}(\phi_A f_q)$ . We emphasize that this term is highly nonlinear (hence the functional dependence of  $\mu_{\text{CORR}}$  on  $\phi_A$ ; however, as demonstrated in Figure 2  $\mu_{\text{CORR}} < 0$  for most values of  $\phi_A$ . For the situations in Figure 3,  $\Delta\mathcal{F}_{\text{CORR}}(f_q, \phi_A) < 0$  since in general  $\mu_{\text{CORR}}(\phi_A = 1) < \mu_{\text{CORR}}(\phi_A < 1)$ . The magnitude of this effect is on the order of as much as  $10k_B T$ , demonstrated in Figure 2, with the direction of this effect schematically illustrated in Figure 4b. This will drastically enhance phase separation, especially at low values of  $\phi_A$  where the difference between  $\mu_{\text{CORR}}(\phi_A = 1)$  and  $\mu_{\text{CORR}}(\phi_A)$  is large. The cumulative effect of  $\Delta\mathcal{F}_{\text{IG}}$  and  $\Delta\mathcal{F}_{\text{CORR}}$  is illustrated in the schematic phase diagram in Figure 4c that demonstrates the effects shown in Figures 4a and b.

This behavior can be conceptually understood as a competition between the Coulombic cohesion, which represents the tendency of local ion structures to order, and counterion/chain entropy. At  $\chi N = 0$ , the translational entropy of both the chains (which is small) and the counterions (which is the primary contribution) tends to drive the system toward mixing such that all components sample the entire system volume. However, there is a strong dependence of the free energy on charge density such that the chain charges and counterions will tend to aggregate due to Coulombic attractions that arise due to correlations. This competition drives phase separation even in the absence of  $\chi$  due to the net attractive nature of the Coulombic interactions but only if these are strongly coupled (large  $\Gamma$ ).

In conclusion, we have shown that upon inclusion of ion correlation effects in the SCFT calculation of polyelectrolyte blends where the Bjerrum length is large ( $\lambda_B/(2a) = 4–25$ ) these correlation effects can have a profound effect on the phase behavior of the system. We have intentionally left out effects such as dielectric self-energy effects, which are known to have pronounced effects on polyelectrolyte blends, to emphasize the magnitude of this particular effect; a full description of a material may need to include such physics.<sup>13</sup> Even in the absence of this effect, at short-range repulsion  $\chi N = 0$  there is a possibility for strong correlation-induced phase separation due to the Coulombic cohesion among the polymer-based charges and their counterions. We have presented these effects in the context of polyelectrolyte blends, which are widely used in the study of ionomer systems.<sup>5</sup> These calculations and results also have profound implications for other inhomogeneous polyelectrolyte systems as well, such as block copolymers that are candidate materials for battery membranes.<sup>12,13,27</sup> Likewise, stimuli-responsive systems are currently of great interest.<sup>11</sup> The electrostatic effects presented here provide a route to tune material properties; however, such design requires an understanding of the thermodynamics of charge correlations.

## AUTHOR INFORMATION

### Corresponding Author

\*E-mail: m-olvera@northwestern.edu.

### Notes

The authors declare no competing financial interest.

## ACKNOWLEDGMENTS

The authors acknowledge support from NSF grant number DMR-0907781. CES thanks the Northwestern International Institute for Nanotechnology for an International Institute for

Nanotechnology Postdoctoral Fellowship. The computational cluster is funded by the Office of the Director of Defense Research and Engineering (DDR&E) and the Air Force Office of Scientific Research (AFOSR) under Award no. FA9550-10-1-0167.

## REFERENCES

- (1) Choi, J.; Rubner, M. F. *Macromolecules* **2005**, *38*, 116–124.
- (2) Pifritis, D.; Tirrell, M. *Soft Matter* **2012**, *8*, 9396–9405.
- (3) Wang, W.; Liu, W.; Tudryn, G. J.; Colby, R. H.; Winey, K. I. *Macromolecules* **2010**, *43*, 4223–4229.
- (4) Bolintineanu, D. S.; Stevens, M. J.; Frischknecht, A. L. *Macromolecules* **2013**, *46*, 5381–5392.
- (5) Zhou, N. C.; Xu, C.; Burghardt, W. R.; Composto, R. J.; Winey, K. I. *Macromolecules* **2006**, *39*, 2373–2379.
- (6) Zhou, N. C.; Burghardt, W. R.; Winey, K. I. *Macromolecules* **2007**, *40*, 6401–6405.
- (7) Lu, X.; Weiss, R. A. *Macromolecules* **1992**, *25*, 6185–6189.
- (8) Smitha, B.; Sridhar, S.; Khan, A. J. *Membr. Sci.* **2005**, *259*, 10–26.
- (9) de Gennes, P. G. *J. Chem. Phys.* **1980**, *72*, 4756–4763.
- (10) Fredrickson, G. H. *The Equilibrium Theory of Inhomogeneous Polymers*; Clarendon Press: Oxford, 2006.
- (11) Walish, J. J.; Fan, Y.; Centrone, A.; Thomas, E. L. *Macromol. Rapid Commun.* **2012**, *33*, 1504–1509.
- (12) Ruzette, A. V. G.; Soo, P. P.; Sadoway, D. R.; Mayes, A. M. *J. Electrochem. Soc.* **2001**, *148*, A537–A543.
- (13) Wang, Z.-G. *J. Phys. Chem. B* **2008**, *112*, 16205–16213.
- (14) Nakamura, I.; Balsara, N. P.; Wang, Z.-G. *Phys. Rev. Lett.* **2011**, *107*, 198301.
- (15) Wang, Q.; Taniguchi, T.; Fredrickson, G. H. *J. Phys. Chem. B* **2004**, *108*, 6733–6744.
- (16) Netz, R. R.; Orland, H. *Eur. Phys. J. E* **2000**, *1*, 203–214.
- (17) Sing, C. E.; Zwanikken, J. W.; Olvera de la Cruz, M. *Macromolecules* **2013**, *46*, 5053–5065.
- (18) Sing, C. E.; Zwanikken, J. W.; Olvera de la Cruz, M. *Phys. Rev. Lett.* **2013**, *111*, 168303.
- (19) Hansen, J. P.; McDonald, I. R. *Theory of Simple Liquids*, 3rd ed.; Boston: Elsevier, 2006.
- (20) Zwanikken, J. W.; Jha, P. K.; Olvera de la Cruz, M. *J. Chem. Phys.* **2011**, *135*, 064106.
- (21) Marko, J. F.; Rabin, Y. *Macromolecules* **1992**, *25*, 1503–1509.
- (22) Kumar, R.; Muthukumar, M. *J. Chem. Phys.* **2007**, *126*, 214902.
- (23) Yang, S.; Vishnyakov, A.; Neimark, A. V. *J. Chem. Phys.* **2011**, *134*, 054104.
- (24) Wang, J. Y.; Chen, W.; Russell, T. P. *Macromolecules* **2008**, *41*, 4904–4907.
- (25) Local homogeneity and electroneutrality are both assumptions of this model. Correlation behaviors like those shown in Sing et al.,<sup>18</sup> while they contribute greatly to the free energy of the system, have a length scale that we consider to be smaller than the coarse-grained features assumed in the SCFT calculation (i.e., only a few ion radii). The ramifications of relaxing this assumption, which is in principle possible, are unclear.
- (26) *CRC Handbook of Engineering Tables*; CRC Press: Boca Raton, FL, 2003.
- (27) Wanakkule, N. S.; Virgili, J. M.; Teran, A. A.; Wang, Z.-G.; Balsara, N. P. *Macromolecules* **2010**, *43*, 8282–8289.